Title
Peptide coated quantum dots for biological applications

Journal
IEEE Transactions On Nanobioscience, 5(4)

ISSN
1536-1241

Authors
Iyer, G
Pinaud, F
Tsay, J
et al.

Publication Date
2006-12-01

Peer reviewed

Peptide Coated Quantum Dots for Biological Applications

Gopal Iyer, Fabien Pinaud, James Tsay, Jack J. Li, Laurent A. Bentolila, Xavier Michalet, and Shimon Weiss*

***Abstract*—Quantum dots (QDOTs) have been widely recognized by the scientific community and the biotechnology industry, as witnessed by the exponential growth of this field in the past several years. We describe the synthesis and characterization of visible and near infrared QDots—a critical step for engineering organic molecules like proteins and peptides for building nanocomposite materials with multifunctional properties suitable for biological applications.**

***Index Terms*—Near infrared (NIR), peptide, quantum dots.**

I. Introduction

THE observation that mineralizing organisms make use of macromolecules such as proteins and lipids to control the nucleation, assembly, and architecture of inorganic phases has opened the door to a new paradigm in nanomaterial design, which has been called molecular biomimetics or biomimetic nanotechnology [1]–[3]. The central premise of this emerging field is that inorganic-binding peptides, either in isolation or when inserted within the structural framework of proteins displaying useful characteristics (e.g., self-assembly or ability to bind other macromolecules such as DNA), can be used as molecular erector sets to direct the assembly of hybrid materials with control of composition and topology [2]. Because naturally occurring biomineralization proteins may only be useful to regenerate the inorganic material that they are associated with, most efforts have been directed at identifying small polypeptides that bind with high affinity to inorganic materials of engineering interest using cell surface or phage display technologies. Although growing, the available "toolbox" of inorganic binding sequences remains small and has been obtained using a limited number of display technologies (chiefly the M13 Ph.D. phage display system commercialized by New England Biolabs, Beverly, MA). Furthermore, little is known about the "rules" governing the interaction between short polypeptides and inorganic compounds. Herein, we discuss the peptide coating of QDOTs and its potential use in biological applications.

Manuscript received May 24, 2006; revised August 8, 2006. This work was supported in part by the U.S. National Institute of Health under Grant NIH 5 R01 EB000312. *Asterisk indicates corresponding author.*

G. Iyer, F. Pinaud, J. Tsay, J. J. Li, L.A. Bentolila, and X. Michalet are with the Department of Chemistry & Biochemistry, University of California at Los Angeles, Los Angeles, CA 90095, USA.

*S. Weiss is with the Department of Chemistry & Biochemistry, California NanoSystems Institute, Department of Physiology University of California at Los Angeles, Los Angeles, CA 90095 USA (e-mail:sweiss@chem.ucla.edu).

Color versions of Figs. 1 and 5–8 are available online at http://ieeexplore.ieee.org.

Digital Object Identifier 10.1109/TNB.2006.886563

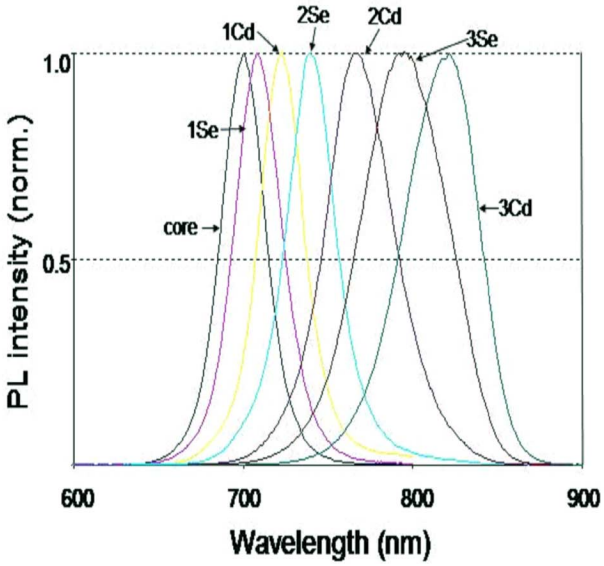

Fig. 1. Normalized photoluminescence emission spectra of core CdTe QDOTs covered with varying CdSe shell. A clear shift from the visible towards the near infrared spectra can be observed by sequential deposition of Cd and Se shell precursors.

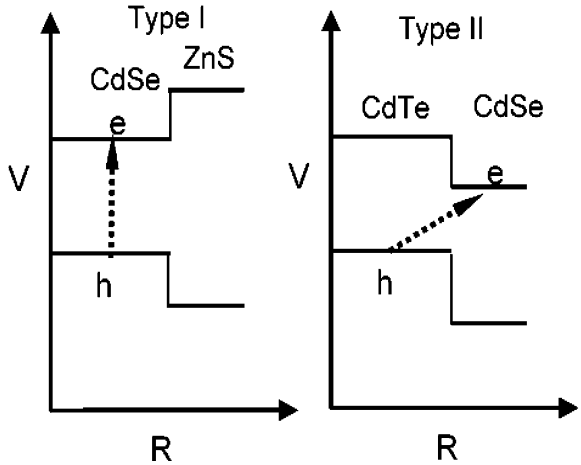

Fig. 2. Left: Band offsets of Type-I CdSe/ZnS QDOTs as a function of distance from the center. Electrons (e−) and holes (h+) stay in CdSe after photoexcitation. Right: Band offsets of Type-II CdTe/CdSe QDOTs as a function of distance from the center. Electrons (e−) are confined in CdSe and holes (h+) confined in CdTe after photoexcitation.

A. Composition and Properties of Visible QDOTs

Colloidal QDOTs consist of an inorganic particle and an organic coating that determines their solubility, functionality, and influences their photophysics QDOTs emitting in the visible range (500–650 nm) and composed of II–VI semiconductor materials are synthesized in our lab following published protocols [4], [5]. These include CdSe cores, CdSe/ZnS and

TABLE I
GRADED CORE SHELLS SHOW SUPERIOR QUANTUM YIELD IN THE ABSENCE AND PRESENCE OF PEPTIDES

Sample	Emission Peak		Quantum Yield (QY)	
	TOP/TOPO (toluene)	peptides (water)	TOP/TOPO (toluene)	peptides (water)
CdSe/ZnS	613	613	19%	9-15%
CdSe/CdS/ZnS (graded)	620	625-630	26%	20-35%
CdSe/CdS/ZnS (layered)	622	624-625	14%	1-2%
CdSe/CdS	620	622-623	35%	2-3%
CdSe/CdS/ZnS (graded)	648	652-654	16%	10-13%

CdSe cores overcoated with inorganic shells of various compositions at different stages of peptide exchange. Ultraviolet annealed graded and peptide coated core shells show higher quantum yield in comparison to layered core shells. All ADOTs (1–3) have identical core sizes (4.5 nm) except sample 4 (CdSe/CdS, 3.5 nm core). Note: sample 5 has a 5×25 nm core.

CdSe/CdS/ZnS core/shell QDOTs. The ratio of cations (group II) to anions (group VI) is maintained at $1:1$. The nucleation and growth of CdSe core and core/shell QDOTs are performed at high temperature in hydrophobic coordinating trioctylphosphine oxide (TOPO) solvents using highly reactive cadmium, selenide, zinc, and sulfur precursors. Synthesis yields are between 80% and 90% and excess precursors are purified out by solvent precipitation and dialysis. A standard synthesis produces about 100 mg of core material that is then coated with shells to give 30 ml of final QDOT solution in hydrophobic solvents at 5 μM. Various QDOT compositions and sizes cover the range 500 nm to 1.7 μm. They have typical (symmetric) emission widths of 25–35 nm [full width at half maximum (FWHM)] in the visible region of the spectrum and large extinction coefficients in the visible and ultraviolet range ($\sim 10^5$ $M^{-1}cm^{-1}$). Many sizes of nanocrystals may therefore be excited with a single wavelength of light, resulting in many emission colors that may be detected simultaneously.

B. Composition of Near Infrared-Emitting (NIR) QDOTs

Various types of QDOTs emitting in the NIR region have attracted much interest for *in vivo* biological imaging [6], [7]. We have also successfully developed NIR emitting QDOTs in our lab (Fig. 1). These include CdTe cores, CdTe/CdSe, CdTe/CdSe/ZnS, and CdTe/CdSe/CdS/ZnS core/shell emitting between 750 and 900 nm. III–V elements such as In, P, and As might also be used for the synthesis of NIR InP, InAs and InAsP QDOTs (Fig. 1) and are currently in the development phase in our lab. The near-infrared type-II CdTe colloidal quantum dots are the result of combination of wave-function engineering concept and layer-by-layer colloidal epitaxy synthetic methods (SILAR) [8]. Nucleation and growth of CdTe QDOTs are done in octadecene with tellurium and cadmium precursors. Similar to visible QDOT synthesis, NIR QDOT synthesis yields are between 80 and 90%. Three- to six-nanometer CdTe core nanocrystals are then coated with two to five monolayers of CdSe to generate high intensity NIR emission. Subsequently, three to five monolayers of ZnS are grown to provide both chemical and photo stability, as well as to minimize the potential toxicity from cadmium leakage. The synthesized type-II NIR QDOTs are readily solubilized and functionalized with synthetic or recombinant peptides developed in our lab.

1) Advantages of NIR QDOTs as Image Contrast Probes: The sensitivity of cell and *in vivo* fluorescence imaging is limited by absorption, scattering, and background fluorescence, which is very strong in the visible part of the light spectrum. In the visible range, fluorescence imaging is limited by the autofluorescence in the visceral tissues, and scattering and absorption in the skin. However, in the nearinfrared (NIR) region, between 700 and 900 nm, hemoglobin absorption drops, and water absorption is low [7], [9], [10]. This increases the transmission of light into and out of deep tissue, thereby improving sensitivity. Imaging with NIR fluorescent probes helps minimize the background from tissue autofluorescence, which decreases with increasing excitation wavelength [11]. Detection of folate-receptor targeted in tumor mice models based on optically quenched near infrared fluorescence (NIRF) probes have enhanced the detection of tumors [12]. Other experiments using optically quenched NIRF probes were able to generate strong NIRF signal after enzyme activation by tumor-associated proteases *in vivo* [13], [14]. However, no good organic fluorophores exist in the NIR range and tumor imaging by NIRF relies extensively on the attachment of multiple organic fluorophores to obtain sufficient signal.

In order to exploit the lack of autofluorescence in the NIR spectrum, the choice of wavelength of the NIR QDOT and the scatter of living tissue is critical for the synthesis of an optimal biocompatible NIR QDOT. For instance, in rat skin, scatter is proportional to $\lambda^{-2.8}$ [15] suggesting a strong wavelength dependence [7] while in postmenopausal human breast, the scatter is proportional to $\lambda^{-0.6}$ [16], suggesting weak wavelength dependence [7]. It is evident from published data that a working

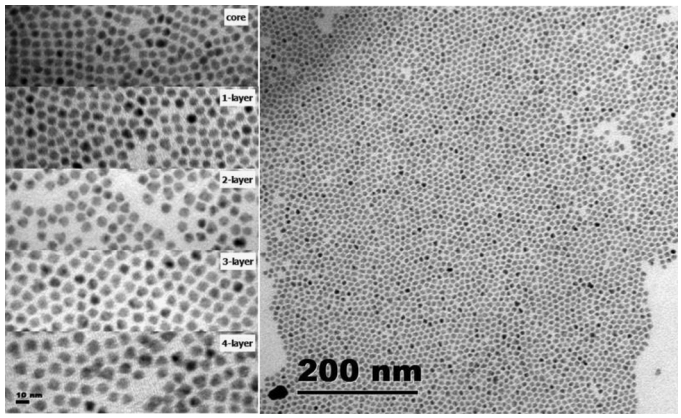

Fig. 3. Left: TEM pictures of CdTe QDOTs covered with varying CdSe shell. Right: TEM of a superlattice formed by CdTe/CdSe with three monolayers of CdSe.

knowledge of the thickness of tissue, photon attenuation (sum of attenuation due to absorbance and scatter) is a prerequisite to optimize the appropriate wavelength of NIR QDOTs for imaging of tumor tissues.

Hence, with the appropriate choice of composition and size, QDs can be synthesized to emit in the NIR. NIR QDs should afford imaging deep in living tissue due to low absorbance and scattering in the NIR wavelength region. In particular, NIR QDs such as CdTe/CdSe can be synthesized with precise control in size using successive ion layer adsorption and reaction (SILAR). [8] These type-II QDs emit light in the NIR due to their indirect band gaps (they have a staggered band alignment, which lowers the energy of emission (Fig. 2). Since color tuning is achieved by controlling the QD size, the chemical synthesis and conjugation chemistry of the different color probes is identical, vastly simplifying matching colors to an application.

C. Engineering Shells for Optimal Photoluminescence and Peptide Interaction

In 1998 we introduced QDOTs as a new class of fluorophores that have many advantages over conventional dyes [17]. QDOTs have been widely recognized by the scientific community and the biotechnology industry, as witnessed by the exponential growth of this field in the past seven years [18]. Below we summarize some of results obtained in our lab. For QDOTs to be biocompatible, they must be water-soluble, nontoxic to the cell, and offer conjugation chemistries for attaching recognition molecules to their surfaces. In addition they should efficiently interphase and bind to biomolecules, target biomolecules of interest, be chemically stable, and preserve their high photostability. We have adhered to standard synthesis procedure of QDOTs in the lab described below.

Two coating steps are necessary to render CdSe cores synthesized in organic solvents highly luminescent, water-soluble, and biocompatible. The first coating step is the chemical deposition of higher bandgap inorganic shells over QDOT cores [19]–[21]. These shells, such as ZnS, serve as isolation layers, protecting the exciton wavefunction from nonradiative recombination processes at surface traps. This shell deposition results in a dramatic enhancement of the luminescence quantum yield. The second coating step utilizes ligand exchange such as

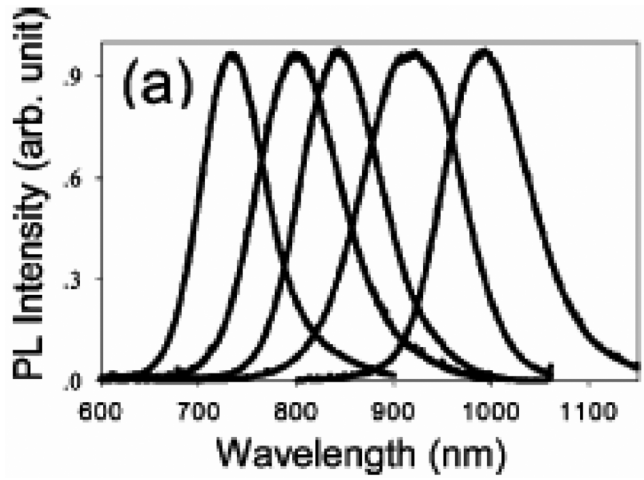

Fig. 4. Normalized room-temperature photoluminescence spectra of different CdTe/CdSe (core/shell) QDOTs. The CdTe core radii and CdSe shell thicknesses are 16 Å/19 Å (core radius/shell thickness) 16 Å/32 Å, 32 Å/11 Å, 32 Å/24 Å, and 56 Å/19 Å from left to the right in the spectra.

silanization [17], [22], mercaptoalkanoic acid ligands [23], organic dendrons [24], amphiphilic polymers [25], phospholipid micelles [26], and oligomeric phosphines [27] to functionalize the hydrophobic QDOTs with an amphiphilic organic layer that serve as an interface between the QDOTs and aqueous solutions.

A novel method developed in our lab for the critical surface ligand exchange steps for QDOTs using peptides will be described in Section I-F below.

D. Shell Composition Effects on Quantum Yield of QDOTs

Reports of increased quantum yield (QY) in QDOT samples possessing a graded CdS/ZnS shell with reduced lattice mismatch led us to look at the cumulated effects of graded/layered shells and peptide coating. Table I summarizes our results: peptide-coating and UV annealing of a graded shell sample allows an almost complete recovery of the original QY, with the graded shell resulting in the higher QY. An additional effect worth noticing is the slight red shift of the emission spectra upon peptide coating of the graded and layered shell samples, indicating a possible interaction between the excitonic wavefunction and the peptide molecular orbitals. Experiments performed with

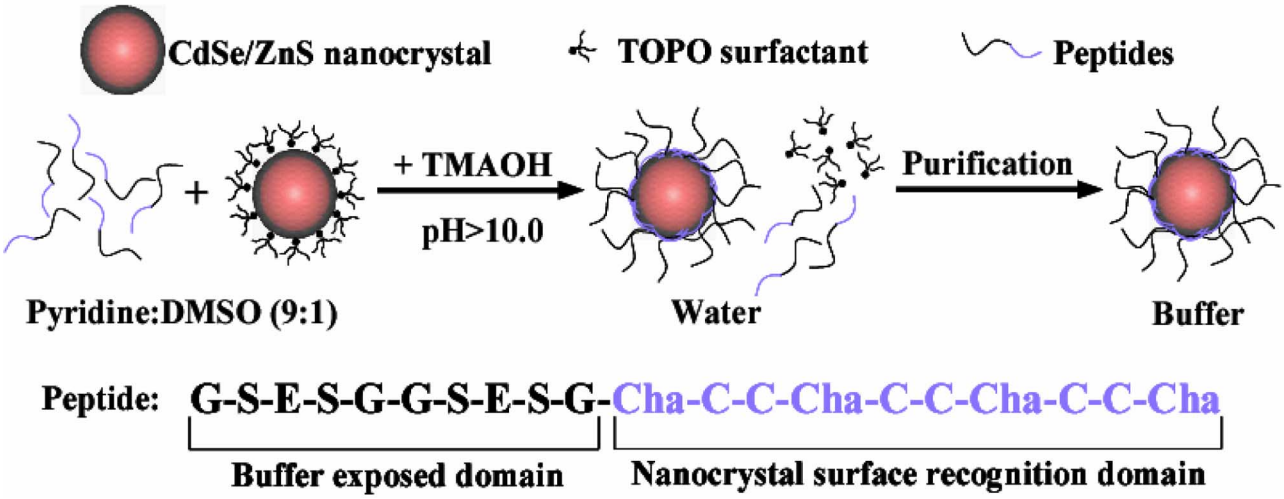

Fig. 5. Surface coating chemistry of CdSe/ZnS QDOTs with phytochelatin-related α-peptides. Box contains the reactants necessary for producing the final product - peptide coated QDOTs. prodTMAOH: Tetramethylammonium hydroxide; Cha: 3-cyclohexylalanine.

peptide sequences containing the same adhesive module and different hydrophilic linkers showed no differences, indicating that only the amino acids in close contact with the shell play a role in this spectral shift. This led us to propose that these pc-QDOTs are amenable to molecular evolution for improved properties, a strategy that has proven extremely powerful for the recognition, synthesis and self-assembly of QDOTs [28], [29]. The composition of shells overcoating CdSe QDOT cores was shown to strongly affect the photoluminescence of the QDOTs after the organic surface (TOPO) were exchanged with phytochelatin-related peptides. CdSe/CdS, layered shell CdSe/CdS/ZnS, graded shell CdSe/CdS/ZnS, and CdSe/ZnS were overcoated with peptides and measured for their QYs (Table I). The varying QY losses after peptide exchange on QDOTs with different compositions/structures of inorganic shells can be clearly seen. Table I demonstrates that graded shell CdSe/CdS/ZnS QDOTs were clearly the optimal QDOTs to use for peptide coating and were most amenable to enhancement with UV irradiation to yield the highest final QYs, out of all the QDOTs studied.

E. Development of Superior NIR-Emitting Semiconductor QDOTs

Biological imaging should especially be enhanced with infrared probes due to increased separation from autofluorescence background and increased penetration of excitation and emission light through tissue. Below we summarize the strategy employed to synthesize QDOT particles that have strong photoluminescence in the IR region: the hybrid approach for CdHgTe/ZnS QDOTs and the SILAR method for Type-II CdTe/CdSe QDOTs.

1) Synthesis of NIR QDOTs By SILAR: The ability to synthesize almost-perfect artificial quantum structures afforded the engineering of confined electronic wavefunctions in a manner never possible before. In the past, two-dimensional (2-D) quantum well structures formed a perfect "laboratory" for the exploration of fundamental quantum mechanical phenomena. Now, the ability to synthesize zero-dimesional

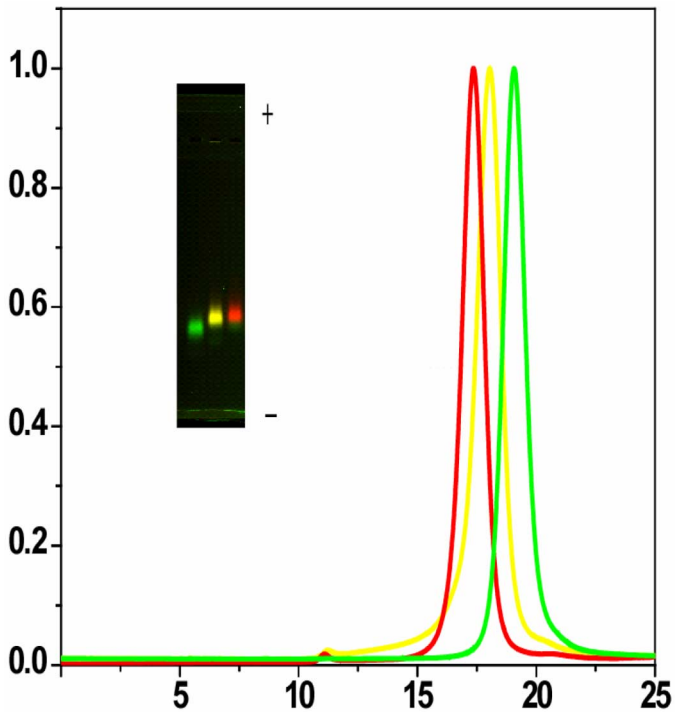

Fig. 6. (a) Gel electrophoresis of green (530 nm), yellow (565 nm) and red (617 nm) CdSe/ZnS QDOTs. (b) Size exclusion HPLC separation of the same three pc-QDOTs. The diameter of the pc-QDOTs calculated from elution volumes: 129.4 Å (15%), 150.3 Å (16%), and 164.8 Å (14%) for the green, yellow, and red samples, respectively.

artificial quantum heterostructures in solution gives us the opportunity to apply wavefunction engineering relevant for biological applications. In particular, we have engineered type-II band alignment so that they may emit in the NIR region, which is of interest for *in vivo* imaging.

Most QDOTs used for biological labeling are visible-emitting type I structures of cores and core/shell QDOTs in which both the electron and hole wavefunctions are mostly confined to the core after excitation beyond the bandgap energy. In contrast, core/shell type-II semiconductor QDOTs have band offsets

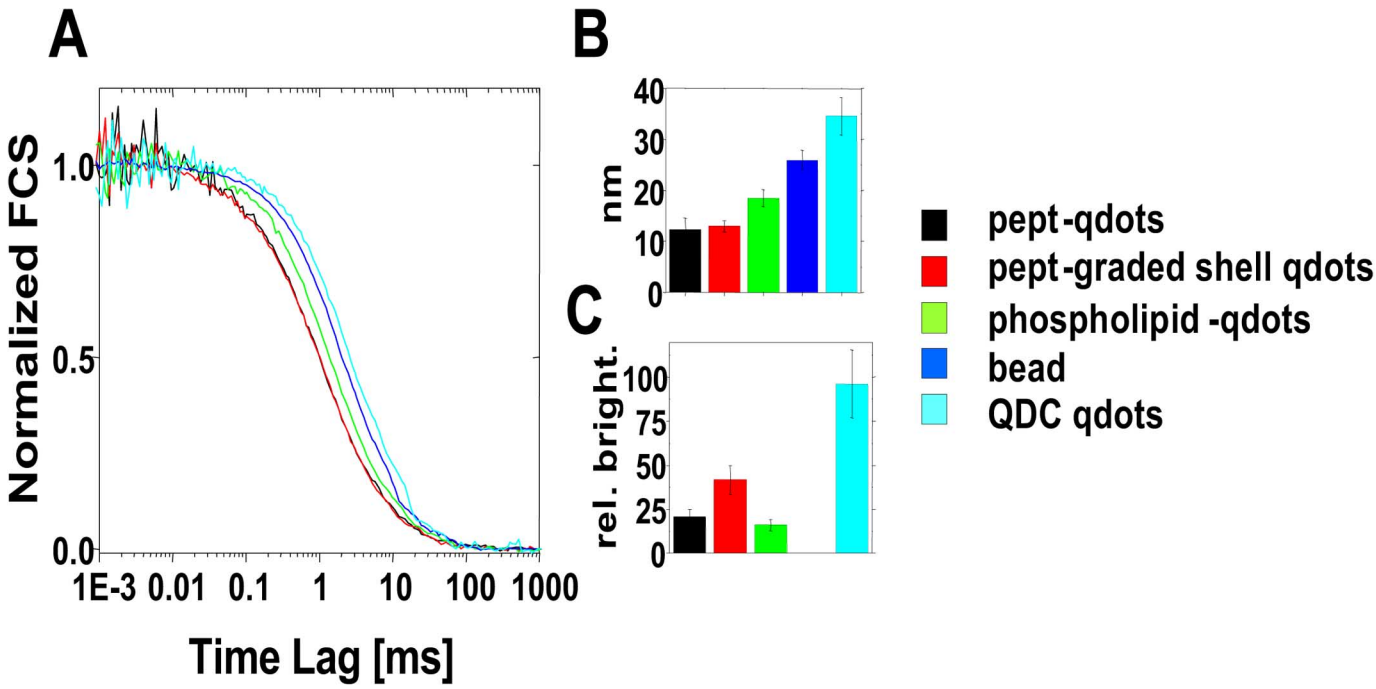

Fig. 7. Fluorescence correlation spectroscopy of various QDOT samples. (A) Normalized FCS curves. black: pc-CdSe/ZnS, red: pc-CdSe/ZnCdS, green: phospholipids coated CdSe/ZnS, dark blue: 25 nm bead, light blue: 605nm Quantum Dot Corp. FCS fits provide (B) hydrodynamic diameter (nm) and (C) brightness per particle (relative brightness). A missing histogram for bead is deliberate in (C) as fluorescence intensity measurement is not necessary due to its extreme bright fluorescence.

between the core and shell resulting in the spatial separation of electron and hole wavefunctions after excitation. Because of their indirect band structures, photoluminescence emissions shift from the visible range in CdTe core QDOTs to the near IR (Fig. 3) with increasing thickness of CdSe shell. These QDOTs are usually characterized by both their red-shifted emissions compared to CdTe and their longer fluorescence lifetimes. Current methods to synthesize these types of QDOTs in solution utilize dangerous precursors and yield materials with larger size distributions and smaller QYs than desired. Their emissions cover a larger spectral range than desired, making it difficult to have multicolor imaging without spectral overlap. In order to synthesize higher quality NIR QDOTs, we employed a method that allows layer-by-layer molecular epitaxy in solution. SILAR utilizes less dangerous precursors and allows half monolayer control of the shell grown on top of the cores, producing particles with excellent size distributions (Fig. 3) and QYs. Briefly, CdTe cores are prepared by mixing Se-TBP (tributylphosphine) with Cd-TDPA (CdO converted with tetradecylphosphonic acid) in 1-Octadecene at high temperature (230 °C–320 °C). Following a brief purification by extraction, CdTe is reloaded into the reaction flask with oleic acid and octadecene. The temperature is raised to 130 °C–270 °C after degassing the system. Calculated amounts of Cd and Se precursor solutions for the corresponding layer are injected alternatively towards the desired number of layers. An optional second shell (CdS or ZnS) could be overgrown in the same way. These CdTe/CdSe QDOTs show strong photoluminescence ranging from 700 to 1000 nm depending on the core size and shell thickness. The QYs of type-II emissions above 800 nm are up to 50% in organic solvents.

2) Absorption/Photoluminescence Spectra of NIR QDOTs: To study the effects of shell growth on fixed size cores, CdTe cores of 5.9 nm diameter were coated with one, two, three, or four monolayers of CdSe shell. There are clear differences in the absorption spectra of CdTe with additional monolayers of CdSe. The absorption peaks continually redshift and lose their definition after each additional injection of shell precursors. After the addition of three shell monolayers, the excitonic features are completely lost. The spatially indirect nature of type-II transitions is responsible for the weaker absorption at the band edges. The photoluminescence emission spectra of CdTe/CdSe were also taken with the same series of different shell thickness samples from a single reaction (Fig. 4). As more layers of CdSe are deposited on CdTe cores, the emission of the QDOT redshifts, originating from the spatially indirect bandedge transition. This redshifted emission gives a direct measure of the energy difference between the valence band edge of CdTe and the conduction band edge of CdSe. The high QY and narrow emissions indicate that the NIR emission from SILAR prepared CdTe/CdSe is not from trap state photoluminescence. Large redshifts of both the absorption profile and photoluminescence emission with additional layers of CdSe provide evidence that type-II QDOTs have been indeed synthesized. The SILAR method described better control over shell compositions and structures because precursors are injected and adsorb on the surface half a monolayer at a time. This method is also compatible with many ligand systems such as amines, phosphines, phosphine oxides, and carboxylic acids. This precise control allows tailoring the interaction between type-II QDOTs and their environment and optimizing photophysical properties. The resultant inorganic NIR QDOTs were also peptide-coated rendering them water-soluble, monodisperse, and bioconjugatable.

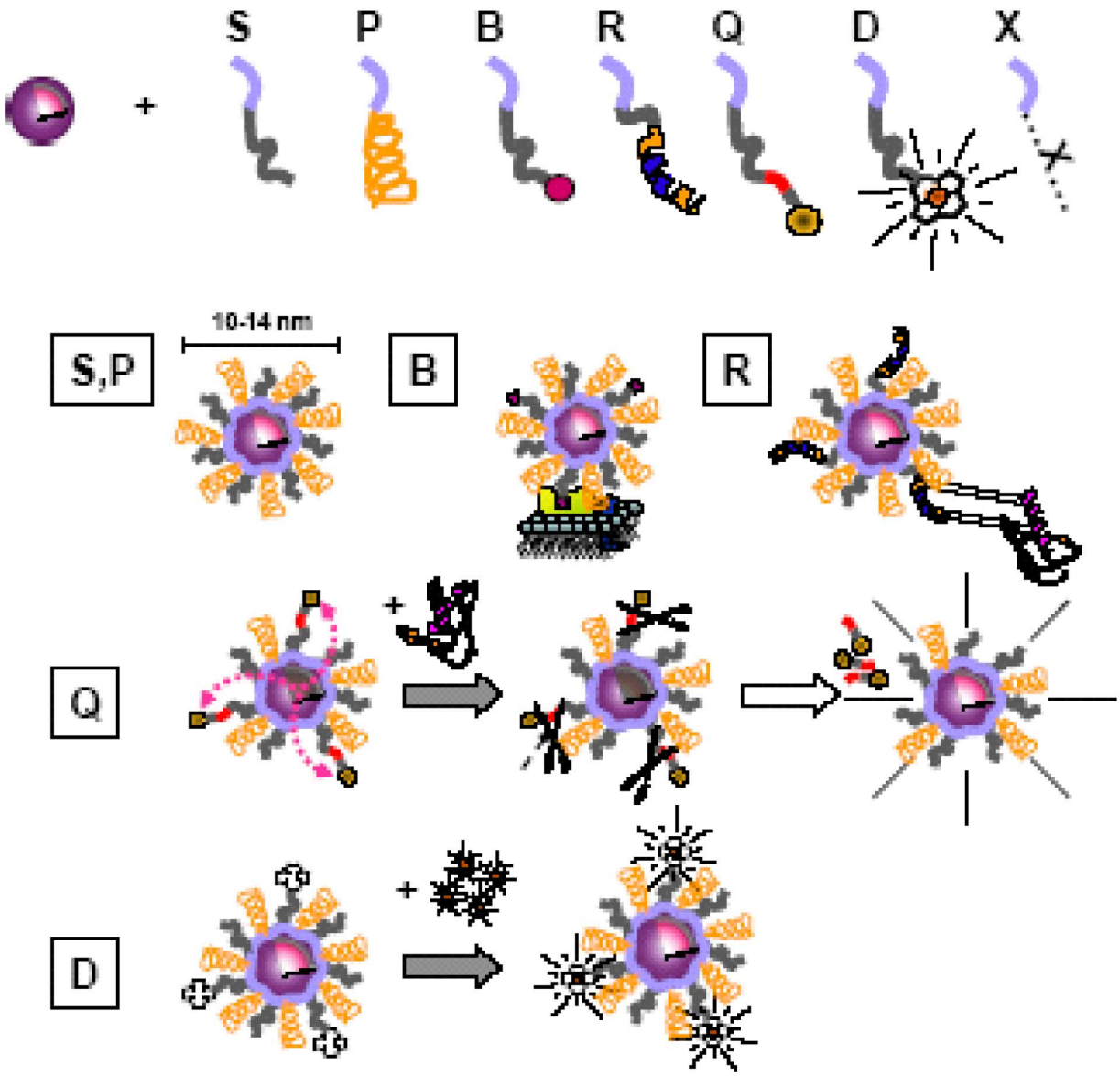

Fig. 8. Peptide "toolkit." Boxed segment contains necessary reactants to make a monofunctional to multifunctional QDOT. The purple segment is common to all peptides and contains cysteines and hydrophobic amino acids. S: solubilization sequence, P: PEG (stabilization), B: biotin, R: recognition/targeting sequence, Q: quencher, D: DOTA (1,4,7,10-tetraazacyclododecane-1,4,7,10-tetraacetic acid) for radionuclide and nuclear spin label chelation. (B) or using peptide recognition sequences (R), or chemical moieties. Quencher linked to QDOT (Q) via a cleavable peptide link. Chelation of PET/MRI probes achieved by DOTA.

F. Peptide Coating and Functionalization of Semiconductor QDOTs

We employed two strategies to solubilize and functionalize QDOTs: silanization and peptide-coating. Initially, we have used a number of ligands to functionalize the nanocrystals [21], and ultimately settled with a thin polymerizable shell of siloxanes to completely coat the nanocrystals and introduce functional groups onto the surface [22], similar to strategies published for gold and CdS nanocrystals [30], [31]. Atomic force microscopy (AFM) and electron energy-loss spectrometry (EELS) microscopy indicated that the siloxane shell was 2–4 nm thick yielding a final particle size of 10–15 nm. High-performance liquid chromatography (HPLC) and 0gel electrophoresis suggested that the solution was composed of ~90% of monomers and dimmers, however, with a wide charge distribution. This approach was successful at introducing thiol and/or amine functional groups while preserving the quantum yield. Using this strategy, QDOTs have been covalently conjugated to a number of biological reporter molecules, including small molecules, proteins, antibodies, and nucleic acids [32] and successfully used in biological *in vitro* assays [32], [33]. However, we found that the reproducibility of the silanization technique was not good, that the size distribution of the particles significantly increased after the modification of the surface and that the wide charge distribution on the QDOTs surface was responsible for considerable non-specific binding that will impair their use in biological *in vivo* labeling experiments. Because of these shortcomings, we developed an alternative approach that attempted to "disguise" QDOTs into soluble proteins. This was

achieved by covering the QDOT's shell surface with synthetic peptides [34] that mimicked the natural formation of peptide-coated QDOTs (pc-QDOTs) during heavy metal detoxification processes in plants and yeasts [35]–[38]. These so-called phytochelatin related peptides had been used as templates for *in vitro* nucleation and growth of ZnS or CdS QDOTs [38], [39]. Inspired by these naturally occurring organic–inorganic hybrid materials, we rationally designed synthetic phytochelatin-like peptides that solubilize and bioactivate tri-n-octylphosphine oxide (TOPO)-coated CdSe/ZnS in aqueous buffer. These peptides comprise a metal-chelating and hydrophobic domain ensuring binding to the QDOT surface, and a hydrophilic tail that provide solubilization and stability in buffers. A single binding domain of the peptide containing cysteines (C) and hydrophobic unnatural amino acids such as 3-cyclohexylalanines (Cha) is responsible for surface recognition and attachment to QDOTs, while the variable more hydrophilic domain provides solubilization and functional groups.

This surface chemistry is achieved in a single reaction step (Fig. 5). The binding of the peptides on the ZnS layer is triggered by forming cysteine thiolates anions with the addition of tetramethylammonium hydroxide (TMAOH) base. Upon binding of the peptides, the nanoparticles precipitate out of the co-solvent, and are redissolved in dimethylsulfoxide (DMSO) and water. The excess of unbound peptides is then removed by dialysis or centrifugal filtration and the purification is assessed by size exclusion liquid chromatography (SE-HPLC) and SDS-PAGE gel electrophoresis (Fig. 6). This approach: 1) protects the core-shell QDOT from degradation; 2) solubilizes QDOTs in aqueous buffer; 3) maintains the original QDOTs photophysical properties; 4) provide a biological interface to QDOTs; 5) allows multiple functions to be easily incorporated; and 6) maintains the overall size of the QDOTs relatively small (8–13 nm). The resulting particles have excellent colloidal and photophysical properties, and are biocompatible as proven by ensemble and single molecule spectroscopy, HPLC, gel electrophoresis, AFM, transmission electron microscopy (TEM), FCS and fluorescence antibunching [34]. Fig. 6 shows that three sizes of peptide-coated CdSe/ZnS QDOTs could be separated on a SE-HPLC column. This separation by size was also observed by gel electrophoresis where the QDOTs have different relative migration distances (Fig. 6). The narrow bands in the gels and the Gaussian shape of SE-HPLC elution peaks reflect narrow size distribution of pc-QDOTs, indicating uniform coating with lack of aggregation (confirmed by AFM and TEM studies) as opposed to the first generation of silanized QDOTs. It was also shown that pc-QDOTs are stable between pH 4.0–10.0, and their photophysical properties (absorption and emission spectra) are unchanged after peptide coating [34]. An important outcome/advantage is their superior inertness since the pc-QDOTs show minimal aggregation and nonspecific binding [40]. Finally, one of the most interesting observations relevant to this proposal is that the peptide coating results in the smallest particles ($\sim$12 nm, compared to $\sim$18 nm for phospholipid-coated QDOTs, and 30 nm for commercial QDOTs protected by a polymer coat as shown in Fig. 7 as assessed by FCS.

II. Summary

A. Towards a "Peptide Toolkit" for the Generation of Multifunctional QDOT Nanocomposite

As discussed above, one of the advantages of the peptide approach relies on those QDOT surface properties that are easily controlled and tuned by reacting various peptide-coating combinations (Fig. 8). The peptide exchange chemistry can be modified to produce a large variety of functional groups that are exposed at the particle surface, allowing a number of covalent modification techniques for conjugation. In general, the presence of amines and/or thiols on the QDOT surface allows for most common conjugation strategies [41], [42] and sidesteps the need to chemically prepare specialized linker molecules. For example, one can easily activate pc-QDOTs with biotin. The QDOTs could be activated via the direct coating of the particles with synthesized biotinylated peptides or via the conjugation of amine reactive biotinylation reagents (such as succinimidyl ester biotin) on a terminal lysine amino acid residue of pc-QDOTs. These QDOT/biotin conjugates show excellent reactivity with streptavidin [34]. Importantly, this bioactivation approach maintains small diameter particles and is particularly suitable for targeting and detecting individual proteins in a living cell. For example, QDOT/biotin conjugates were used to target avid in fusion to glycosylphosphatidyl-inositol CD14 cell surface receptor (CD14-Av) in cultured HeLa cells [34]). This approach demonstrated the specific recognition of the CD14-Av proteins on the cell membrane. The brightness and high saturation intensity of pc-QDOTs [40], [43] allows the use of an inexpensive CCD camera (CoolSnap *cf*, Princeton Instruments, Trenton, NJ) and rather short exposure time (100 ms). This gives access to the high-resolution spatial and temporal information afforded by single-molecule fluorescence tracking, but also to the very high-resolution structural information, unique to electron microscopy.

In conclusion, the preliminary results generated in our lab have successfully demonstrated a QDOT solubilization approach based on the rational design of peptide modules accomplishing different functions: NC surface recognition, solubilization, functionalization and targeting [43]. This trial and error approach has led to the discovery of a few peptide sequences having a common surface recognition sequence (SRS) containing tandem repeats of a Cha–Cys–Cys motif, where Cha is cyclohexyl-alanine, an unnatural AA. There are several advantages of using peptide chemistry: 1) (natural and unnatural) peptide chemistry is well established and automated; 2) the catalog of physicochemical properties of individual amino acids is almost limitless; 3) the resulting coating layer helps camouflaging the inorganic NC and reducing its recognition as a foreign object by the cell; and 4) molecular evolution techniques can be used to screen the enormous phase space of possible properties.

References

[1] M. Sarikaya, "Biomimetics: Materials fabrication through biology," *Proc. Nat. Acad. Sci. USA*, vol. 96, pp. 14 183–14 185, 1999.

[2] M. Sarikaya, C. Tamerler, A. K.-Y. Jen, K. Schulten, and F. Baneyx, "Molecular biomimetics: Nanotechnology through biology," *Nature Mater.*, vol. 2, pp. 577–585, 2003.

[3] N. C. Seeman and A. M. Belcher, "Emulating biology: Building nanostructures from the bottom up," *Proc. Nat. Acad. Sci. USA*, vol. 99 Suppl 2, pp. 6451–6455, 2002.
[4] C. B. Murray, D. J. Norris, and M. G. Bawendi, "Synthesis and characterization of nearly monodisperse CdE (E = S, Se, Te) semiconductor nanocrystallites," *J. Amer. Chem. Soc.*, pp. 8706–8715, 1993.
[5] C. V. Bowen Katari JE and Alivisatos AP, "X-ray photoelectron spectroscopy of CdSe nanocrystals with applications to studies of the nanocrystal surface," *J. Phys. Chem.*, vol. 98, pp. 4109–4117, 1994.
[6] B. Ballou, B. C. Lagerholm, L. A. Ernst, M. P. Bruchez, and A. S. Waggoner, "Noninvasive imaging of quantum dots in mice," *Bioconjug. Chem.*, vol. 15, pp. 79–86, 2004.
[7] S. Kim, Y. T. Lim, E. G. Soltesz, A. M. De Grand, J. Lee, A. Nakayama, J. A. Parker, T. Mihaljevic, R. G. Laurence, D. M. Dor, L. H. Cohn, M. G. Bawendi, and J. V. Frangioni, "Near-infrared fluorescent type II quantum dots for sentinel lymph node mapping," *Nature Biotechnol.*, vol. 22, pp. 93–97, 2004.
[8] J. J. Li, Y. A. Wang, W. Z. Guo, J. C. Keay, T. D. Mishima, M. B. Johnson, and X. G. Peng, "Large-scale synthesis of nearly monodisperse CdSe/CdS core/shell nanocrystals using air-stable reagents via successive ion layer adsorption and reaction," *J. Amer. Chem. Soc.*, vol. 125, pp. 12 567–12 575, 2003.
[9] A. H. Hielscher, A. Y. Bluestone, G. S. Abdoulaev, A. D. Klose, J. Lasker, M. Stewart, U. Netz, and J. Beuthan, "Near-infrared diffuse optical tomography," *Dis. Markers*, vol. 18, pp. 313–337, 2002.
[10] E. M. Sevick-Muraca, J. P. Houston, and M. Gurfinkel, "Fluorescence-enhanced, near infrared diagnostic imaging with contrast agents," *Curr. Opin. Chem. Biol.*, vol. 6, pp. 642–650, 2002.
[11] Y. T. Lim, S. Kim, A. Nakayama, N. E. Stott, M. G. Bawendi, and J. V. Frangioni, "Selection of quantum dot wavelengths for biomedical assays and imaging," *Mol. Imag.*, vol. 2, pp. 50–64, 2003.
[12] W. K. Moon, Y. Lin, T. O'Loughlin, Y. Tang, D. E. Kim, R. Weissleder, and C. H. Tung, "Enhanced tumor detection using a folate receptor-targeted near-infrared fluorochrome conjugate," *Bioconjug. Chem.*, vol. 14, pp. 539–45, 2003.
[13] R. Weissleder, C. H. Tung, U. Mahmood, and A. Bogdanov, Jr, "In vivo imaging of tumors with protease-activated near-infrared fluorescent probes," *Nature Biotechnol.*, vol. 17, pp. 375–8, 1999.
[14] M. F. Kircher, R. Weissleder, and L. Josephson, "A dual fluorochrome probe for imaging proteases," *Bioconjug. Chem.*, vol. 15, pp. 242–8, 2004.
[15] W. F. Cheong, S. A. Prahl, and A. J. Welch, "A review of the optical properties of biological tissues," *IEEE J. Quantum Electron.*, vol. 26, no. 12, pp. 2166–2185, Dec. 1990.
[16] A. E. Cerussi, A. J. Berger, F. Bevilacqua, N. Shah, D. Jakubowski, J. Butler, R. F. Holcombe, and B. J. Tromberg, "Sources of absorption and scattering contrast for near-infrared optical mammography," *Acad. Radiol.*, vol. 8, pp. 211–8, 2001.
[17] M. P. J. Bruchez, "Luminescent semiconductor nanocrystals—Intermittent behavior and use as fluorescent biological probes," in *Chemistry*, 1998.
[18] J. J. Li, J. M. Tsay, X. Michalet, and S. Weiss, "Wavefunction engineering: From quantum wells to near-infrared type-II colloidal quantum dots synthesized by layer-by-layer colloidal epitaxy," *Chem. Phys.*, vol. 318, pp. 82–90, 2005.
[19] M. A. Hines and P. Guyotsionnest, "Synthesis and characterization of strongly luminescing Zns-capped CdSe nanocrystals," *J. Phys. Chem.*, vol. 100, pp. 468–471, 1996.
[20] B. O. Dabbousi, J. RodriguezViejo, F. V. Mikulec, J. R. Heine, H. Mattoussi, R. Ober, K. F. Jensen, and M. G. Bawendi, "(CdSe)ZnS core-shell quantum dots: Synthesis and characterization of a size series of highly luminescent nanocrystallites," *J. Phys. Chem. B*, vol. 101, pp. 9463–9475, 1997.
[21] X. G. Peng, M. C. Schlamp, A. V. Kadavanich, and A. P. Alivisatos, "Epitaxial growth of highly luminescent CdSe/CdS core/shell nanocrystals with photostability and electronic accessibility," *J. Amer. Chem. Soc.*, vol. 119, pp. 7019–7029, 1997.
[22] D. Gerion, F. Pinaud, S. C. Williams, W. J. Parak, D. Zanchet, S. Weiss, and A. P. Alivisatos, "Synthesis and properties of biocompatible water-soluble silica-coated CdSe/ZnS semiconductor quantum dots," *J. Phys. Chem. B*, vol. 105, pp. 8861–8871, 2001.
[23] W. C. W. Chan and S. M. Nie, "Quantum dot bioconjugates for ultrasensitive nonisotopic detection," *Science*, vol. 281, pp. 2016–2018, 1998.
[24] W. Z. Guo, J. J. Li, Y. A. Wang, and X. G. Peng, "Conjugation chemistry and bioapplications of semiconductor box nanocrystals prepared via dendrimer bridging," *Chem. Mater.*, vol. 15, pp. 3125–3133, 2003.
[25] D. R. Larson, W. R. Zipfel, R. M. Williams, S. W. Clark, M. P. Bruchez, F. W. Wise, and W. W. Webb, "Water-soluble quantum dots for multiphoton fluorescence imaging in vivo," *Science*, vol. 300, pp. 1434–1436, 2003.
[26] B. Dubertret, P. Skourides, D. J. Norris, V. Noireaux, A. H. Brivanlou, and A. Libchaber, "In vivo imaging of quantum dots encapsulated in phospholipid micelles," *Science*, vol. 298, pp. 1759–1762, 2002.
[27] S. Kim and M. G. Bawendi, "Oligomeric ligands for luminescent and stable nanocrystal quantum dots," *J. Amer. Chem. Soc.*, vol. 125, pp. 14 652–14 653, 2003.
[28] S. R. Whaley, D. S. English, E. L. Hu, P. F. Barbara, and A. M. Belcher, "Selection of peptides with semiconductor binding specificity for directed nanocrystal assembly," *Nature*, vol. 405, pp. 665–668, 2000.
[29] S.-W. Lee, C. Mao, C. E. Flynn, and A. M. Belcher, "Ordering of quantum dots using genetically engineered viruses," *Science*, vol. 296, pp. 892–895, 2002.
[30] L. M. Lizmarzan, M. Giersig, and P. Mulvaney, "Synthesis of nanosized gold-silica core-shell particles," *Langmuir*, vol. 12, pp. 4329–4335, 1996.
[31] M. A. CorreaDuarte, M. Giersig, and L. M. LizMarzan, "Stabilization of CdS semiconductor nanoparticles against photodegradation by a silica coating procedure," *Chem. Phys. Lett.*, vol. 286, pp. 497–501, 1998.
[32] D. Gerion, W. J. Parak, S. C. Williams, D. Zanchet, C. Micheel, and A. P. Alivisatos, "Sorting fluorescent nanocrystals using DNA," *J. Amer. Chem. Soc.*, vol. 124, pp. 7070–7074, 2002.
[33] D. Gerion, F. Chen, B. Kannan, A. Fu, W. J. Parak, D. J. Chen, A. Majumdar, and A. P. Alivisatos, "Room-temperature single nucleotide polymorphism and multi-allele DNA detection using fluorescent nanocrystals and microarrays," *Anal. Chem.*, vol. 75, pp. 4766–4772, 2003.
[34] F. Pinaud, D. King, H. P. Moore, and S. Weiss, "Bioactivation and cell targeting of semiconductor CdSe/ZnS nanocrystals with phytochelatin-related peptides," *J. Amer. Chem. Soc*, vol. 126, pp. 6115–23, 2004.
[35] M. J. Stillman, "Metallothioneins," *Coordination Chem. Rev.*, vol. 144, pp. 461–511, 1995.
[36] C. S. Cobbett, "Heavy metal detoxification in plants: Phytochelatin biosynthesis and function," *IUBMB Life*, vol. 51, pp. 183–188, 2001.
[37] C. T. Dameron, R. N. Reese, R. K. Mehra, A. R. Kortan, P. J. Carroll, M. L. Steigerwald, L. E. Brus, and D. R. Winge, "Biosynthesis of cadmium sulphide quantum semiconductor crystallites," *Nature*, vol. 338, pp. 596–597, 1989.
[38] C. T. Dameron and D. R. Winge, "Peptide-mediated formation of quantum semiconductors," *Trends Biotechnol.*, vol. 8, pp. 3–6, 1990.
[39] W. Bae and R. K. Mehra, "Metal-binding characteristics of a phytochelatin analog (Glu-Cys)(2)Gly," *J. Inorganic Biochem.*, vol. 68, pp. 201–210, 1997.
[40] S. Doose, J. M. Tsay, F. Pinaud, and S. Weiss, "Comparison of photophysical and colloidal properties of biocompatible semiconductor nanocrystals using fluorescence correlation spectroscopy," *Anal. Chem.*, vol. 77, pp. 2235–2242, 2005.
[41] A. Waggoner, "Covalent labeling of proteins and nucleic acids with fluorophores," *Methods Enzymol.*, vol. 246, pp. 362–73, 1995.
[42] G. Hermanson, *Bioconjugate Techniques*. San Diego, CA: Academic, 1996.
[43] X. Michalet, F. F. Pinaud, L. A. Bentolila, J. M. Tsay, S. Doose, J. J. Li, G. Sundaresan, A. M. Wu, S. S. Gambhir, and S. Weiss, "Quantum dots for live cells, *in vivo* imaging, and diagnostics," *Science*, vol. 307, pp. 538–44, 2005.

Authors' photographs and biographies not available at the time of publication.